ResearchGate

See discussions, stats, and author profiles for this publication at: https://www.researchgate.net/publication/8183260

Study of soft tissue cutting forces and cutting speeds

Article *in* Studies in health technology and informatics · February 2004

DOI: 10.3233/978-1-60750-942-4-56 · Source: PubMed

CITATIONS
22

READS
1,296

3 authors, including:

Teeranoot Chanthasopeephan
King Mongkut's University of Technology Thonburi
13 PUBLICATIONS **232** CITATIONS

SEE PROFILE

All content following this page was uploaded by Teeranoot Chanthasopeephan on 11 December 2014.

The user has requested enhancement of the downloaded file.

Study of Soft Tissue Cutting Forces and Cutting Speeds

Teeranoot CHANTHASOPEEPHAN, Jaydev P. DESAI, and Alan C. W. LAU
Program for Robotics, Intelligent Sensing, and Mechatronics (PRISM) Laboratory
3141 Chestnut Street, MEM Department, Room# 2-115
Drexel University
Philadelphia, PA 19104
{teeranoo, desai, alau}@coe.drexel.edu

Abstract: *A versatile equipment to study the cutting of soft tissue with surgery scalpel was designed and constructed. Experiments were performed with pig liver (ex-vivo) to measure the blade-tissue interaction forces at cutting speeds ranging from 0.1 cm/sec-2.54 cm/sec. The experimentally measured force-displacement curves reveal that the liver cutting process was made up of a sequence of repeating local units with similar features. Each local unit was comprised of a linear deformation phase followed by a crack growth phase. A method was developed to quantify the deformation resistance of the tissue during each local deformation phase in cutting. This deformation resistance was presented in the form of a self-consistent local effective Young's modulus (LEYM), and was determined by post-processing force-displacement data with finite element models. Values for LEYM were determined from plane-stress finite element model and plane-strain finite element model. The plane-stress LEYM values were within a close bound of the plane-strain values. Results of the self-consistent LEYM at different cutting speeds show that the tissue's resistance to deformation decreased as the cutting speed increased.*

1. Introduction

Estimation and modeling of soft tissue deformation during cutting is important for developing a reality based haptic interaction model for surgical training and simulation. In our ongoing study, we are interested in incorporating the cutting parameters (such as the cutting speed) in the predictive model that is self-consistent with the experimental observations. In particular, we are interested in hepatic (liver) tumor biopsies and simulating the cutting forces for surgical resident training and surgical simulation. The liver is composed of lobules held together by an extremely fine areolar structure and covered by a serous and a fibrous coat. Tumors appearing in the liver are either primary or secondary tumors. While electrocautery and ultrasonic dissection are the most preferred approach for cutting in liver surgery, our surgeon collaborators indicate that there are specific circumstances where the use of a scalpel is necessary. One of those specific circumstances is liver biopsies. Cutting with a scalpel allows better identification of margins without cellular distortion (as is caused in electrocautery). The surgeon should have opportunities to practice and familiarize themselves with the complexities of a surgical procedure before operating on patients. As a result, it is necessary to develop models based on actual experimental data. Our goal is thus to develop a

model of soft tissue interaction with a cutting blade while working with the liver in particular. In the literature, most modeling efforts are focused towards assuming the mechanical properties and developing methods to efficiently solve the tissue simulation problem for robot-assisted surgery / training.

Modeling of deformable tissues is critical for providing accurate haptic feedback to the surgeon in common surgical tasks such as grasping, cutting, and dissection. Models constructed through FEM, for example, should be able to accurately represent the surgical task based on the physics of the task. Current approaches to modeling deformation of organs are either geometry-based or physics-based. In geometry-based methods, the deformations are purely based on geometric manipulations without considering the dynamic interactions within the object. Physics-based models simulate the physical behavior of objects and involve the internal and external forces. Significant work in geometry-based models using either the vertex-based approach [1] or spline-based [2] approach has been done. Physics based models are computationally more intensive and utilize particle-based schemes [3], finite element method [4, 5], or meshless methods [6]. However, most of these methods assume a linear elastic model and hence the computations are done offline before the actual simulation begins. Linear elastic models do not represent an accurate model for finite strains; however, it is a good starting point in modeling tissue interaction.

Modeling tissue cutting has also been explored to a limited extent [7]. Most of the work in the literature does not involve the physics behind cutting (such as energy exchange) [8, 9]. Resolved-force haptic devices, such as the PHANToM from SensAble Technologies (Woburn, MA), have been used to display external cutting forces of a single blade in surgical procedures [10]. In addition, cutting with scissors has been modeled, without the display of internal cutting forces [8, 9]. However, there is limited literature on the effect of cutting on global deformations. Scissors cutting data was gathered for biological tissues by Greenish and Hayward, but not modeled [11, 12]. The integration of local grasping forces measured from real tissues into larger global models has not been studied. Recently, there has been some work on modeling cutting in surgery [13, 14, 15].

2. Equipment and Experiment

2.1 Design and development of the soft tissue cutting equipment

The equipment consists of a scalpel-blade cutting subsystem, a computer control subsystem, a digital data-acquisition subsystem, and a data post-processing subsystem (see figure 1). The test equipment to measure the liver cutting forces was designed to have multiple capabilities such as: a) varying the angle of cutting the liver (the machine allows the angle variation from 0 to ±90 degrees), b) adjust the height of the scalpel by moving the cutting mechanism over a vertical column to control the depth of cut (the vertical supports can be adjusted in the range of 30 to 50 cm from the base), and c) variable cutting speed to measure the effect of cutting speed on cutting forces and strain rates within the specimen (speeds can be varied from 0 to 3.81cm/second). The constrained boundary shown in the figure was designed to simulate the attachment of the liver on one end as in a human body (such as the attachment to the diaphragm). The cutting mechanism consists of two vertical supports, a lead screw assembly with a geared DC motor and an incremental encoder (manufactured by Maxon Motors, model A-max32 with planetary gearhead GP 32C and digital encoder HEDL 55 with line driver RS 422), and a JR3 precision 6-axis force/torque sensor (model 85M35A-I40, with worst case resolution of 0.05 N in Fx and Fy, 0.1 N in Fz and 0.00315 Nm in Tx, Ty and Tz) to which a surgeon's scalpel is attached. We used #10 Bard-Parker stainless steel surgical blade in our experimental studies, consistent with what is used by surgeons.

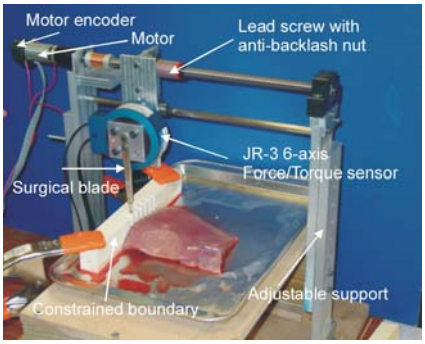

Figure 1. Experimental setup for measuring the cutting forces in the pig liver.

The cutting blade traversed linearly based on the rotary motion of the DC motor. An anti-backlash nut connected the lead screw to the force sensor. The scalpel was screwed to the force sensor and the force sensor was mounted on an aluminum plate with one end attached to the anti-backlash nut traveling along the lead screw and the other end on a lower guiding shaft (parallel to the lead screw) with a linear bearing to provide low friction linear travel. The assembly was designed to provide 20cm of travel distance for cutting the liver specimen. The design and construction of the cutting assembly ensured that the system was sufficiently rigid with no backlash so that the forces recorded by the force sensor are those obtained by cutting the tissue alone. The dSPACE DS1103 controller board (manufactured by dSPACE, Inc.) recorded the position and force data from the motor's encoder and force sensor in real-time. We have implemented a proportional + derivative (PD) controller to enable precise movement of the motor (and hence the cutting blade during cutting tasks).

2.2 Experimental procedure for measuring tissue cutting forces

Since the experiments were performed on ex-vivo liver tissue, the preparation of the tissue before the experiment helped maintain the properties of the tissue as close as possible to the in-vivo properties. To maintain the properties, we transported the liver from freshly slaughtered pigs to our laboratory within 2 hours post mortem. During the experimental setup, the liver was placed on a bed of saline soaked gauze, sprayed with saline and sealed in a container. The liver tissue sample was not preconditioned because in surgery, the cutting forces experienced by the surgeon are on non-preconditioned tissues.

Before starting the experiment, we cut the pig liver into specimens of size 8x12x2.5 cm. The outer encapsulated surface was not cut since we were interested in measuring the cutting forces on the liver. The outer rim of the specimen was covered with petroleum jelly to minimize moisture loss during the experiment. A bar of rectangular shape made of machineable plastic with an array of small nails clamped at the bottom end penetrated through one edge of the liver specimen to simulate a single constrained boundary surface. While this is not an exact replication of the boundary conditions for a human liver (which is partially attached on one end to the diaphragm) this is none-the-less a valid simplification for our initial tests and model (based on our discussions with surgeon collaborators).

Each liver sample (size of 8x12x2.5 cm) could accommodate four parallel cutting lines. During the cutting process, we obtained the force versus distance from the constrained boundary characteristics of liver tissue. We used the JR3 force sensor to measure the X, Y, and Z components of the cutting force and the norm of these forces was plotted versus the displacement of the cutting blade. Experiments were performed with three cutting speeds, namely 0.1cm/sec (quasi-static cutting speed), 1.27cm/sec (intermediate cutting speed), and 2.54 cm/sec (normal cutting speed). We conducted 12 liver cutting experiments for each cutting speed.

3. Results

3.1 Characteristics of the cutting force curve

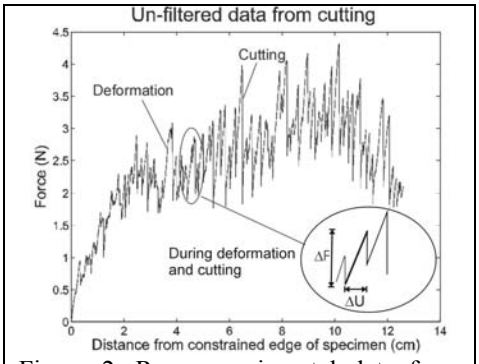

Figure 2. Raw experimental data from liver cutting. Typical repeating units of linear loading segment followed by sudden unloading segment are shown.

The cutting force versus cut-length data reveal that the overall curve is made up of many repeating local units of similar feature (Figure 2). Each local unit is comprised of a deformation phase followed by a crack growth phase, and is portrayed (Figure 2 insert) as a segment of linear loading followed by a segment of sudden unloading respectively. In each repeating unit the cutting force increased linearly to a higher magnitude during tissue deformation. Then the force suddenly dropped as onset of localized crack growth occurred in the tissue. In the experiments, each visually observed localized blade cut on the tissue clearly corresponded to a sudden drop of the force measured by the force sensor. A filtering procedure was developed to post-process the data to cleanly identify the "hilltops" and "valleys" of the sequence of local loading and unloading in the force versus cut-length curve.

3.2 Quantifying the resistance to deformation

It is desirable to construct a predictive computational model that can simulate the cutting process (each local deformation and crack growth phases) and predict the mechanical response (overall cutting force versus cutting-blade displacement curve) of liver cutting. The cutting process has two repeating phases: local deformation and local crack growth. In this section, we provide a measure for the deformation resistance of the tissue during the local deformation phase in the cutting process. The measure we use is the *local effective Young's modulus* (LEYM) that is *self-consistent* with experimental data and finite element method (FEM) simulation models.

To be of real-time application, a simulation model should not be computationally intensive. For this purpose, we propose to use two-dimensional finite element (FE) models instead of a three-dimensional model. A plane-strain FE model is most appropriate for simulating the cutting of thick liver specimen in which the through-thickness strain can be idealized as negligible. On the other hand, a plane-stress FE model is appropriate for simulating the cutting of thin liver specimen in which the through-thickness stress can be idealized as negligible. Simulation results from both a plane-stress model and a plane-strain model will bracket the actual mechanical response of liver specimens of various thicknesses.

To simulate the cutting process in a computationally most efficient manner, we would like to use as coarse a FE mesh as possible in the simulation but still be able to predict the actual force-displacement response as would be measured by the experiments. This can be accomplished by using the LEYM that is self-consistent with experimental data and the coarse-mesh FE model. A systematic method to derive this LEYM is as follow:

A typical finite element model of the liver specimen was constructed with 4-noded quadrilateral elements, using the ANSYS software (Version 6.1). The Young's modulus of a biological tissue is not constant and it can vary from location to location [16]. To simulate each of the linear loading segments (see Figure 2 insert for example), we conducted linear elastic FE analysis with Poisson's ratio 0.3 and an initial local effective Young's modulus of arbitrary magnitude E_1. Then we applied the experimentally-measured ΔU^{exp} (see insert of Figure 2) of that loading segment to the FE node that modeled the cutting blade. We performed the FE analysis and compared the FEM computed force ΔF^{FEM} of that node to the

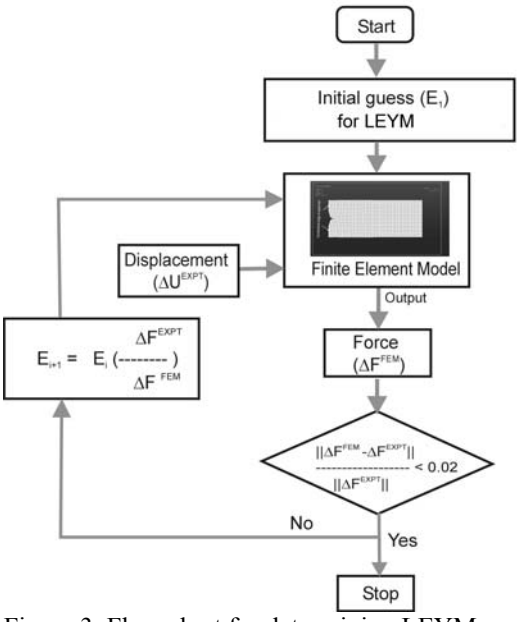

Figure 3. Flow chart for determining LEYM.

experimentally measured ΔF^{exp}. In the first iteration, ΔF^{FEM} will not be equal to ΔF^{exp}, and we systematically updated the new value of the local effective Young's modulus to E_2 and repeated the process, until ΔF^{FEM} of the new iteration was within the neighborhood of the experimentally measured ΔF^{exp}. The final E value so determined is the local effective Young's modulus, $E^{effective}$. We systematically iterated $E^{effective}$ by:

$$E_{i+1} = E_i \left(\frac{\Delta F^{EXPT}}{\Delta F^{FEM}}\right) \qquad for \;\; i = 1,2,..... \qquad (1)$$

The iteration convergence criterion was:

$$\frac{\left\| \Delta F^{FEM} - \Delta F^{EXPT} \right\|}{\Delta F^{EXPT}} \leq 0.02 \qquad (2)$$

This iteration procedure is schematically shown in Figure 3.

In future application, we can construct a FE mesh of the liver, assign the elements in the FE model with their respective $E^{effective}$ and use the FE model to simulate various patterns of liver cutting with varying cutting parameters. Such a FE model embedded with self-consistent LEYM will be able to predict each of the monotonic loading segments in cutting consistent with the experimentally-measured cutting forces and displacements, should actual experiments of those particular cutting patterns and cutting parameters be performed.

3.3 Effect of cutting speed

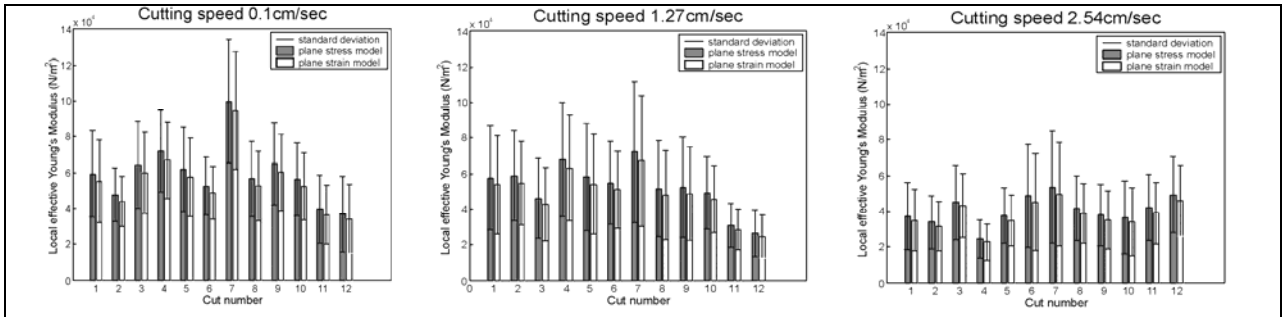

Figure 4. The average of the LEYM of 12 cuts and the corresponding standard deviation at a) 0.1cm/sec cutting speed, b) 1.27cm/sec cutting speed, and c) 2.54cm/sec cutting speed.

The result from varying the cutting speed is shown in Figure 4 and Table 1. We conducted 12 liver cutting experiments for each cutting speed. Results from 12 liver cuttings in each speed revealed that the LEYM varied from location to location in the liver but the spatial variation was within reasonable bounds. Also, the LEYM values from plane-stress analysis were within close bounds to those from plane-strain analysis.

We observed that as the cutting speed increased, the values of LEYM and the corresponding standard deviation decreased. The tissue therefore exhibits an apparently lower resistance to deformation at higher cutting speed. The

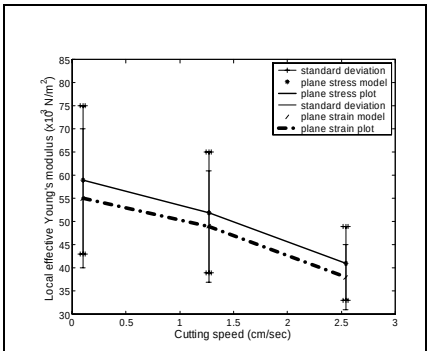

Figure 5. Relationship between the average LEYM and cutting speed.

relationship between the average LEYM and cutting speed appeared to be linear in both plane-stress and plane-strain analyses (Figure 5). The linear model could thus be used to predict the characteristic for the liver tissue during cutting at different speeds.

	Plane stress model V=0.1cm/sec		Plane strain model V=0.1cm/sec		Plane stress model V=1.27cm/sec		Plane strain model V=1.27cm/sec		Plane stress model V=2.54cm/sec		Plane strain model V=2.54cm/sec	
Test #	Average LEYM $x10^3$ N/m^2	Standard deviation $x10^3$ N/m^2	Average LEYM $x10^3$ N/m^2	Standard deviation $x10^3$ N/m^2	Average LEYM $x10^3$ N/m^2	Standard deviation $x10^3$ N/m^2	Average LEYM $x10^3$ N/m^2	Standard deviation $x10^3$ N/m^2	Average LEYM $x10^3$ N/m^2	Standard deviation $x10^3$ N/m^2	Average LEYM $x10^3$ N/m^2	Standard deviation $x10^3$ N/m^2
1	59	24	55	23	57	29	53	27	37	19	35	17
2	48	15	44	14	59	25	55	23	34	15	32	14
3	64	24	60	23	46	22	43	21	45	21	43	18
4	72	23	67	21	68	32	63	30	24	11	23	10
5	62	23	57	22	58	30	54	28	37	15	35	14
6	52	16	49	15	55	23	51	22	49	29	45	27
7	100	34	94	33	72	40	67	37	53	31	50	29
8	57	21	53	19	52	27	48	25	42	18	39	17
9	65	23	60	21	52	28	48	26	38	17	35	16
10	56	20	52	19	49	20	46	19	37	21	34	19
11	40	19	37	16	31	12	29	11	42	19	39	17
12	37	21	34	19	26	13	25	12	49	21	46	20
AVG	59	16	55	15	52	13	49	12	41	7.5	38	7

Table 1. Average LEYM at 3 cutting speeds.

4. Conclusions and Future Work

Results from experiments revealed that the cutting process consisted of a sequence of repeating units, with each unit comprising of local deformation phase followed by a local fracture (crack growth) phase. The cutting force versus displacement curve showed repeating units where each unit consisted of a linear loading segment followed by a sudden unloading segment (local fracture). We proposed to use the *local effective Young's modulus* that is self-consistent with experimental data and finite element simulation model as a measure of the deformation resistance of the tissue during the deformation phase. The values of LEYM obtained from plane-stress FEM model for various cutting speeds were close to the corresponding values from plane-strain FEM models. For the purpose of real-time simulation, two-dimensional FEM model embedded with self-consistent LEYM was a good alternative to a three-dimensional model, which was more computationally intensive. Results show that there was a decrease in LEYM and the corresponding standard deviation as the cutting speed increased. This indicated that as the cutting speed increased there was a decrease in the apparent resistance to deformation in cutting. In future work, we plan to perform experiments with additional cutting speeds and vary the cutting angle. We are also developing an apparatus that can measure the depth of the blade in the tissue as the cutting progresses, thereby allowing us to normalize the cutting forces with the depth of cut. Finally, from the past literature in tissue biomechanics, many living tissues exhibit nonlinear and inhomogeneous behavior. Hence, our future work in this area will also focus on developing a nonlinear model that can reproduce the observed cutting forces and localized deformations in this type of soft tissues.

Acknowledgements

We would like to acknowledge the support of National Science Foundation grants EIA-0312709 and CAREER Award IIS-0133471 for this work. The first author would also like to thank the Thai government for supporting her graduate studies. We would also like to thank Dr Andres Castellanos (MD), for providing us with insightful information on liver tumor biopsies.

References

[1] M. A. Srinivasan, "Surface deflection of primate fingertip under line load," *Journal of Biomechanics*, vol. 22, pp. 343-349, 1989.

[2] C. Basdogan, C. Ho, M. A. Srinivasan, S. Small, and S. Dawson, "Force interactions in laparoscopic simulations: Haptic rendering of soft tissues," presented at Proceedings of the Medicine Meets Virtual Reality VI Conference, 1998.

[3] S. A. Cover, N. F. Ezquerra, J. O'Brien, R. Rowe, T. Gadacz, and O. Palm, "Interactively deformable models for surgery simulation," *IEEE Computer Graphics and Applications*, vol. 13, pp. 65-78, 1993.

[4] S. Cotin, H. Delingette, and N. Ayache, "Real-Time elastic deformations of soft tissue for surgical simulation," *IEEE Transactions On Visualization and Computer Graphics*, vol. 5, pp. 62-73, 1999.

[5] C. Basdogan, C. Ho, and M. A. Srinivasan, "Virtual environments for medical training: Graphical and Haptic simulation of common bile duct exploration," *IEEE/ASME Transactions on Mechatronics*, vol. 6, pp. 267-285, 2001.

[6] S. De, J. Kim, and M. A. Srinivasan, "A meshless numerical technique for physically based real-time medical simulations," presented at Proceedings of the Medicine meets virtual reality, 2001.

[7] M. Mahvash and V. Hayward, "Haptic Rendering of Cutting: A Fracture Mechanics Approach," *Haptics-e, The Electronic Journal of Haptics Research*, vol. 2, 2001.

[8] C. B. Ho, M. A. Srinivasan, S. D. Small, and S. L. Dawson, "Force Interaction in Laparoscopic Simulation: Haptic Rendering Soft Tissues," presented at Proceedings of the Medicine Meets Virtual Reality, San Diego, 1998.

[9] G. Picinbono, H. Delingette, and N. Ayache, "Nonlinear and anisotropic elastic soft tissue models for medical simulation," presented at IEEE International Conference on Robotics and Automation, 2001.

[10] K. Hirota, A. Tanaka, and T. Kaneko, "Representation of force in cutting operation," presented at Proceedings of IEEE Virtual Reality, 1999.

[11] S. Greenish, V. Hayward, T. Steffen, V. Chial, and A. M. Okamura, "Measurement, Analysis and Display of Haptic Signals During Surgical Cutting," *Presence*, vol. 11, pp. 626-651, 2002.

[12] S. Greenish, "Acquisition and Analysis of Cutting Forces of Surgical Instruments for Haptic Simulation," in *Department of Electrical and Computer Engineering*: McGill University, 1998.

[13] G. Tholey, T. Chanthasopeephan, T. Hu, J. P. Desai, and A. C. W. Lau, " Measuring Grasping and Cutting Forces for Reality-Based Haptic Modeling," presented at Computer Assisted Radiology and Surgery,17th International Congress and Exhibition, London, UK, 2003.

[14] T. Chanthasopeephan, J. P. Desai, and A. C. W. Lau, "Measuring Forces in Liver Cutting for Reality-Based Haptic Display," presented at IEEE/RSJ International Conference on Intelligent Robots and Systems, Las Vegas, Nevada, 2003.

[15] T. Chanthasopeephan, J. P. Desai, and A. C. W. Lau, "Measuring Forces in Liver Cutting: New Equipment and Experimental Results," *Annals of Biomedical Engineering*, vol. 31, 2003.

[16] Y. C. B. Fung, "Elasticity of soft tissues in simple elongation," *American Journal of Physiology*, vol. 213, pp. 1532-1544, 1967.

View publication stats